

NCC-1-216

Efficient Approximation for Structural Optimization under Multiple Constraints

Final report on NASA Cooperative Agreement
—NCC-1260

Raphael T. Haftka
Department of Aerospace Engineering,
Mechanics & Engineering Science
University of Florida
Gainesville, FL 32611-6250

November 1997

Summary

The cooperative agreement covered work between August 1995 and August 1997. During that time, Dr. Raphael T. Haftka, Dr. John H. Garcelon and Dr. Mehmet Akgün at the University of Florida worked together with Dr. Stephen J. Scotti of the Thermal Structures Branch of the NASA Langley Research Center. The focus of the work was efficient approximations of structural response and sensitivity. The effort proceeded in three directions as follows:

1. Development of an approximation based on work by Kirsch, extended to efficient sensitivity approximations and demonstrated for structural models for the High Speed Civil Transport. A paper on this part was written and presented (Ref. 1). An updated version, Attachment A, was submitted to the AIAA Journal.
2. Preliminary development of the adjoint method for calculating sensitivity derivatives, Attachment B
3. A review of method for fast exact reanalysis, Ref. 2, was submitted to a conference, and a draft is included as Attachment C.

References:

1. Garcelon, J., Haftka, R., and Scotti, S., "Approximation in Optimization and Damage Tolerant Design AIAA Paper 97-1050, Proceedings of the 38th AIAA/ASME/ASCE-/AHS/ASC Structures, Structural Dynamics and Material Conference, Kissimmee, FL, April 7-10, 1997, Part 2, pp. 1193-1203.
2. M. A. Akgün, J. H. Garcelon, and R. T. Haftka "Fast Exact Static Structural Reanalysis in Relation to the Sherman-Morrison-Woodbury Equation," paper submitted to the ISSMO/NASA/AIAA Internet Conference on Approximation and Fast Reanalysis in Engineering Optimization, June 1998.

APPROXIMATIONS IN OPTIMIZATION OF DAMAGE TOLERANT STRUCTURES

John H. Garcelon* and Raphael T. Haftka†
University of Florida, Gainesville, FL 32611

Stephen J. Scotti‡
NASA Langley Research Center
Hampton, VA 23681

Approximations for structural response and design sensitivities significantly reduce the computational cost of structural optimization. To be useful the approximation must be accurate and computationally efficient. Damage tolerant design puts even more stringent computational demands on optimization procedures and approximations due to the large structural changes inherent in damage. A robust approximation is evaluated and extended to include design sensitivities. It is implemented in an optimization procedure and tested. It is shown that this approximation is accurate and efficient for damage tolerant optimum design of complex structural models. Lastly, a qualitative measure is developed and tested that estimates the computational savings using the approximation.

Introduction

Structural optimization often requires a large number of structural analyses, and for complex structures this can become prohibitively expensive. For this reason, it is common to use approximations to the structural analysis during the optimization process to reduce the computational cost. There are two general categories of approximations according to their ranges of applicability in the design space. Global approximations are valid in large regions of the design space, while local approximations are only valid in the vicinity of a point in the design space.¹

Damage tolerant design is defined as a design that can tolerate the destruction of one or more major structural components. In composite aircraft structures, conventional damage tolerant design typically results in a significant mass penalty. However, through optimal design for damage tolerance, this mass penalty can be significantly reduced.²

Damage tolerant design requires a global approximation because of the large changes possible in the response of a damaged structure. The need for an efficient and accurate approximation is particularly acute when structures are designed for improved damage tolerance

since a large number of damage scenarios must be considered to avoid designs tailored to withstand damage at only particular locations. In that case, each structural design has to be evaluated by analyzing the undamaged structure as well as a host of damage configurations under several load cases typically different for the undamaged and damaged cases. In addition, for optimization we usually need the derivatives of the structural response of the undamaged and damaged configurations with respect to the design variables.

Local function approximations are usually based on a series expansion about a point in the design space. Storaasli and Sobieszczanski used the first-order Taylor series for reanalysis of structures with small structural changes.³ Approximate reanalysis was done in a fraction of the time with displacement and stress errors less than 16%. Noor and Lowder found that the first-order Taylor series expansion technique was inaccurate for stiffness changes greater than 20%.⁴ They also considered second-order Taylor series expansions, which they found to be more accurate but at a substantial increase in computational cost.⁵ Taye used a binomial expansion to directly approximate structural response.⁶ The accuracy of the binomial series

* Visiting Assistant Professor, Department of Aerospace Engineering, Mechanics and Engineering Science. (jhg@ce.ufl.edu) Associate Member AIAA.

† Professor, Department of Aerospace Engineering, Mechanics and Engineering Science. (haftka@ufl.edu) Fellow AIAA.

‡ Head, Thermal Structures Branch.

approximation depends on the magnitude of the changes to the structure, making it also a local approximation.

The reduced basis technique is a global approximation that expresses the structural response as a linear combination of known independent vectors. The accuracy of this technique depends on the number and quality of the basis vectors. The number of basis vectors is typically much less than the number of degrees of freedom. Fox and Miura used as basis vectors previously computed displacement vectors obtained from previous changes to the structure.⁷ Kavanagh employed eigenvectors of the original structure.⁸ Only those eigenvectors with a significant energy contribution were included. Noor and Lowder used response first derivatives for basis vectors.⁴ All these basis vectors work well in approximating global changes; however, accuracy is still limited for complex structures, and computational efficiency may still be improved.

Kirsch has developed a combined binomial-reduced basis approximation, which has proved to be highly accurate even for large structural changes in truss structures.⁹ Similar to Noor and Lowder's approach, Kirsch uses the first several terms in the binomial series as basis vectors. He shows good results for changes in the design variables of up to 700%.

The objectives of the present paper are: (a) to investigate the accuracy and efficiency of the combined approximation for complex wing structures under severe damage conditions; (b) to extend the method to approximations of the derivatives of damaged structural response with respect to design variables; (c) to include the approximation procedure together with a sequential approximate optimization method; and (d) to estimate the computational savings that these approximations provide.

The paper begins with a section presenting the problem statement, followed by a summary of the combined approximation. Next the extension of the method to design derivative approximation is presented, a section on the optimization method follows, and two example problems are used to demonstrate the application to realistic models of wing structures.

Problem Statement

Given an undamaged structure's stiffness matrix, \mathbf{K}_0 , and the vector of applied loads, \mathbf{R} , the displacements, \mathbf{u}_0 , can be calculated using the displacement method of analysis

$$\mathbf{K}_0 \mathbf{u}_0 = \mathbf{R}.$$

\mathbf{R} is assumed independent of the stiffness and damage. \mathbf{K}_0 will change due to damage ($\Delta\mathbf{K}$) and the damaged structure's stiffness matrix is,

$$\mathbf{K} = \mathbf{K}_0 + \Delta\mathbf{K}.$$

An exact reanalysis requires solving the modified system of equations for the new displacements, \mathbf{u}_{new} ,

$$\mathbf{K} \mathbf{u}_{\text{new}} = (\mathbf{K}_0 + \Delta\mathbf{K}) \mathbf{u}_{\text{new}} = \mathbf{R}. \quad (1)$$

Combined Approximations

Local approximations are based on series expansions about a baseline stiffness matrix and are accurate for small changes in the matrix. One such local approximation is based on the binomial series,

$$\mathbf{u}_{\text{new}} = \mathbf{u}_0 - \mathbf{K}_0^{-1} \Delta\mathbf{K} \mathbf{u}_0 + [\mathbf{K}_0^{-1} \Delta\mathbf{K}]^2 \mathbf{u}_0 - [\mathbf{K}_0^{-1} \Delta\mathbf{K}]^3 \mathbf{u}_0 + \dots \quad (2)$$

The computational effort and the accuracy of the approximation depend on the number of terms retained in the series.

Global approximations are valid for large changes in the stiffness matrix. In the reduced basis method, the displacement vector, \mathbf{u} , is approximated by a linear combination of n linearly independent displacement vectors. Usually n is a small number.

$$\mathbf{u} \approx q_0 \mathbf{u}_0 + q_1 \mathbf{u}_1 + q_2 \mathbf{u}_2 + \dots + q_{n-1} \mathbf{u}_{n-1} = \mathbf{U}_B \mathbf{q}. \quad (3)$$

\mathbf{U}_B is a collection of the n displacement vectors. Substituting the approximate displacements from equation (3) for \mathbf{u}_{new} in equation (1) and pre-multiplying by \mathbf{U}_B^T yields

$$\mathbf{U}_B^T \mathbf{K} \mathbf{U}_B \mathbf{q} = \mathbf{U}_B^T \mathbf{R}. \quad (4)$$

The reduced stiffness matrix is introduced as

$$\mathbf{K}_R = \mathbf{U}_B^T \mathbf{K} \mathbf{U}_B, \quad (5)$$

and the reduced load vector is

$$\mathbf{R}_R = \mathbf{U}_B^T \mathbf{R}, \quad (6)$$

So that equation (4) becomes

$$\mathbf{K}_R \mathbf{q} = \mathbf{R}_R. \quad (7)$$

The reduced stiffness matrix, \mathbf{K}_R , is $n \times n$ in size, and the reduced load vector, \mathbf{R}_R , is $n \times 1$ in size, where $n \ll m$. The coefficients, \mathbf{q} , are obtained by solving equation (7) and the approximate displacements, \mathbf{u} , are then calculated using equation (3).

The success of the reduced basis method depends on selecting an appropriate set of linearly independent basis vectors, U_B .¹ The selection of basis vectors has been highly problem dependent; however, Kirsch uses the first several terms of a series as basis vectors as does Noor. Kirsch calls this technique Combined Approximations (CA).

Kirsch has demonstrated excellent results using this technique on simple truss and frame problems. We have extended the combined approximation technique by including approximations for structural response derivatives and by applying higher order approximations for more complex structures. Using the binomial series (2), basis vectors u_j , $j=1\dots n-1$ can be generated by using the following recursive relationship, noting that K_0 is available in decomposed form and the first basis vector is the nominal displacements:

$$u_0 - \text{nominal displacements,} \\ K_0 u_j = -\Delta K u_{j-1}, \quad j=1, \dots, n-1. \quad (8)$$

Using this recursive relationship, generating basis vectors is relatively inexpensive computationally, and high order approximations can easily be generated. For the structural models presented in this paper, generation of each basis vector requires 2% of the time required for a complete analysis. A first order approximation uses the first two terms of the binomial series; second and third order approximations use three and four terms, respectively.

Approximation to Design Derivatives of Response With Damage

The previous section described the approximations used for the response of damaged configurations. For the design process we need also the derivatives of the response with respect to changes in structural parameters. This section describes a process that approximates these derivatives.

Consider the displacement approximation given in equation (3), where q are coefficients determined using the CA approach, and u_0 are the exact displacements of the nominal structure. Differentiating with respect to design variable x (denoted using the comma notation,) yields the following equation:

$$u_{,x} \approx U_B q_{,x} + U_{B,x} q = q_{0,x} u_0 + \dots + q_{n-1,x} u_{n-1} + q_0 u_{0,x} + \dots + q_{n-1} u_{n-1,x} \quad (9)$$

The displacement response basis vectors u_0 through u_{n-1} have previously been computed. In addition, $u_{0,x}$, the sensitivity derivative of displacements for the undamaged structure, is normally computed in structural

optimization, and can be calculated using any standard method such as the semi-analytical method shown in equation 10.

$$u_{0,x} = -K_0^{-1} (\Delta K / \Delta x) u_0. \quad (10)$$

The other basis vector derivatives, $u_{1,x}$ through $u_{n-1,x}$, are expensive to calculate and are truncated from equation (9) to yield the following displacement derivative approximation:

$$u_{,x} \approx b_0 u_0 + \dots + b_{n-1} u_{n-1} + b_n u_{0,x} = V_B b, \quad (11)$$

where b are the unknown coefficients. Differentiating the displacement equation (1) with respect to a structural parameter, x , yields

$$(K)_{,x} u + K u_{,x} = 0. \quad (12)$$

Introducing equation (3) and equation (11) into equation (12) gives,

$$K V_B b = -(K)_{,x} U_B q. \quad (13)$$

Premultiplying both sides of equation (13) by V_B^T ,

$$V_B^T K V_B b = -V_B^T (K)_{,x} U_B q. \quad (14)$$

The reduced stiffness matrix is

$$K_R = V_B^T K V_B, \quad (15)$$

and $(K)_{,x}$ is approximated by the finite difference,

$$(K)_{,x} \approx \Delta K / \Delta x. \quad (16)$$

The coefficients, b , can be determined by solving,

$$K_R b = -V_B^T \Delta K / \Delta x U_B q, \quad (17)$$

and the displacement derivative approximated by

$$u_{,x} = V_B b. \quad (18)$$

Using $u_{,x}$, the stress derivatives may be computed. It is important to realize that although the accuracy of the response approximation can be improved by using more basis vectors (equation 8), the accuracy of the design derivatives is influenced by the truncation of equation (9).

Optimization Procedure

The optimization problem calls for minimizing the weight, W , subject to constraints on stresses, buckling, and displacements and is formulated as

$$\text{Minimize } W(x), \\ \text{such that } g_i(x) < 0.$$

where g_i are the constraint functions. The optimization is solved by a sequential linear programming (SLP) procedure, developed by Scotti, which employs both

linear constraint approximations and derivative approximations.¹⁰ In addition, the SLP procedure employs a penalized objective function, P , given as

$$P = W + K \sum_i \max(g_i, 0).$$

Where K is a constant set to be larger than the largest of all Lagrange multipliers of the constraints. This penalized objective ensures that when no feasible solution exists to the linearized problem (possibly due to move limits), the solution found will minimize the magnitude of the constraint violations.

Move limits are incorporated to ensure the accuracy of the linear programming problem. To reduce the number of design variables, design variable linking is used, where the finite element model is partitioned into design regions and within each region, all elements are sized by the same design variables. Additional details of the optimization procedure are given in Appendix A.

EAL Implementation

All computer simulations are done using the EAL analysis language. The optimization procedure described in Appendix A has been implemented using EAL. During development of the optimization procedure and of the approximation algorithm, EAL offered three key features. First, the analysis database is open and can be easily manipulated. Second, EAL provides a powerful command language with state of the art computational features. Third, EAL allows for simple inclusion of user-written FORTRAN subroutines that can interact with the database and be controlled using the command language.

The database features allow both element stiffness and stress-displacement matrices to be easily manipulated. Elements may be grouped such that design variable linking is facilitated. Elements from different groups can be collected into sets, and the resulting set of elements can be manipulated as an entity.¹² For example, damage scenarios are described using this set feature. A set of elements, which may be derived from different groups and element types, represents that

portion of a structure that is damaged. Manipulation of the set allows for those elements' stiffness contribution (ΔK) to be easily identified and modified.

The EAL command language provides a rich set of linear algebra and sparse matrix operations. This provides a good environment for prototyping, testing, and implementation. Damage is modeled as reduced or eliminated structural stiffness. The stiffness of the structure, in sparse form, is directly manipulated to reflect the damage for each design condition. Likewise, element stress-displacement matrices are manipulated for damaged elements prior to constraint evaluation. Several FORTRAN routines are used to generate data, such as the local buckling constraints, that are too complicated, or computationally inefficient to be implemented using the command language. Although the EAL code was used for the present approximation development, it is important to note that implementation of the approximation could be done in most finite element codes that utilize the displacement method of analysis.

EAL provides CPU utilization information for evaluation of computational efficiency. As implemented, the optimization procedure can disable the use of approximations for the damaged conditions. This allows for comparison between the approximate analysis and a complete reanalysis. The following example problems use this feature to estimate the accuracy and efficiency of the approximation.

Example Problems

Two example problems illustrate the accuracy and efficiency of the method. First, a simple model of the High Speed Civil Transport (HSCT) shows the effects of the approximation order on accuracy of the approximations near large area wing damage. The second example problem is a finely meshed box beam model, which demonstrates how accuracy and efficiency of the approximations are affected as the model size increases. In addition, the box beam model is used in a full optimization using the approximation.

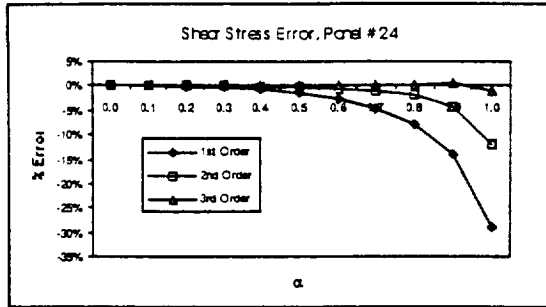


Figure 4: Shear Stress Error vs. Damage Magnitude.

Figure 4 shows the shear stress error in the skin panel #24. Skin panel #24 is located near the fuselage, adjacent to the damaged area. The improvement in accuracy of the third order approximation compared to the lower order approximations is much more dramatic for this element. The third order approximation with less than a 3% stress error is much more accurate than first and second order approximations. Reducing the stress and displacement approximation errors is important when considering approximating design derivatives of response.

Table 1: Design Derivative Approximations

	Panel #24, shear stress	
	$d\tau / dx$	$d(\log \tau) / d(\log x)$
Central Diff.	272749	0.028
Approximation	367060	0.037
	Rib #78, axial stress	
	$d\sigma / dx$	$d(\log \sigma) / d(\log x)$
Central Diff.	128192	1.72
Approximation	119810	1.61
	Panel #163, normal stress	
	$d\sigma_{xx} / dx$	$d(\log \sigma_{xx}) / d(\log x)$
Central Diff.	221382	0.62
Approximation	242030	0.58

Table 1 shows a comparison of the approximate derivative of several typical stress components with respect to the top wing panel design variable. Table 1 also shows the magnitudes of the derivatives and logarithmic derivatives from both the difference approximation and the approximation method proposed in this work. The logarithmic derivative represents the ratio of the fractional change in the function to the fractional change in the variable. For example, a logarithmic derivative ($d(\log \sigma) / d(\log x)$) of 0.03 indicates that a 1% change in x will lead to a 0.03% change in σ . When the logarithmic derivative is much smaller than unity, the sensitivity of the parameter is small and the derivative is difficult to evaluate accurately. As can be seen from the large differences in the derivative approximated by the different methods for panel #24 and the correspondingly low values for the logarithmic derivative, the accuracy of either of

these methods may be poor. The design derivative approximations for rib cap #78 and panel #163 show much better correlation with the difference approximation, and both have much larger logarithmic derivatives than those of panel #24. Rib cap #78 and panel #163 are also in the vicinity of the damage. A third order approximation using 4 basis vectors was used to generate these design derivative approximations.

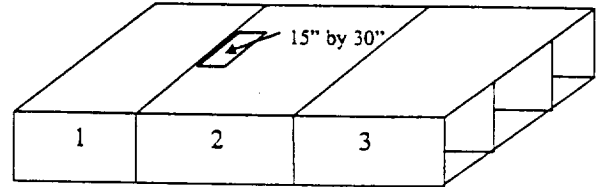


Figure 5: Design Regions and Top Surface Damage Location for the Box Beam Model

Box Beam Test Cases

The next model is a 180-inch by 90-inch portion of a 3-bay, titanium honeycomb wing box beam. This model consists of 5,978 nodes, 480 2-node bar elements representing spar caps, and 6,000 plate bending elements representing the titanium honeycomb. There are a total of 29,561 degrees of freedom in this model. Two load cases are considered that correspond to 2.5g and -1.0g maneuvers, respectively. There are three design variable regions, shown in Figure 5, dividing the beam evenly lengthwise for a total of 24 design variables. The design variables consist of the spar cap areas and the face sheet gauges and honeycomb core depths of the webs, upper surface, and lower surface. Each design region is optimized for minimum weight subject to strength and panel buckling constraints. These result in 12,481 constraints. All subsequent results are calculated at the optimum design conditions.

First, the accuracy of the approximation was examined. Both the constraint and constraint sensitivities were computed and compared with those calculated by performing a complete reanalysis. A single load condition corresponding to a 2.5g maneuver and a single damage case were used. The damage considered was debonding of a 15-inch by 30-inch section of the bottom surface in the center bay 2. The approximation was run using 2, 3, 4, and 5 displacement response basis vectors generated using equation 8. These same basis vectors are used for the response derivative approximations along with the $u_{0,x}$ basis vector as in equation 11.

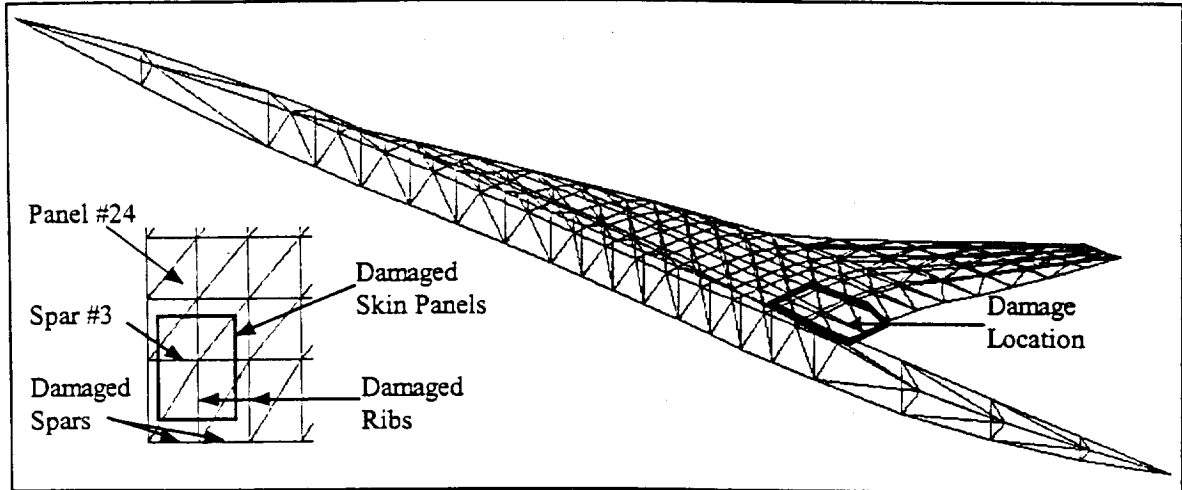


Figure 1: Simple HSCT Model.

Simple HSCT Test Case

Figure 1 shows a simple model of the High Speed Civil Transport (HSCT). This is a relatively coarse half model with 193 nodes, 449 2-node bar elements, 383 membrane elements, and 129 shear panel elements for a total of 533 degrees of freedom. A single load case was used that simulates a 2.5g pull-up maneuver. The damage considered consisted of a complete loss of structural stiffness for the top wing skin panels from the connected ribs and spars at the wing's trailing edge, next to the fuselage. The damage was simulated by removing 8 membrane elements for the top wing skin panels and 4 bar elements for the spar and rib caps in this area of the wing. A single design variable for the top wing panel thickness around the damage area was considered. The design variable is associated with 22 triangular membrane elements that include the 8 damaged membrane elements.

As a global measure of the accuracy of the approximation, the potential energy of the approximate analysis is compared to that of a complete reanalysis. In order to track the error, the stiffness of the damaged elements are gradually reduced to zero by a factor, $(1 - \alpha)$, so that α can be viewed as a damage magnitude measure. First, second, and third order approximation errors are shown in Figure 2. Although all three approximations show a small global error, the accuracy of the approximations can only be truly assessed at the local level.

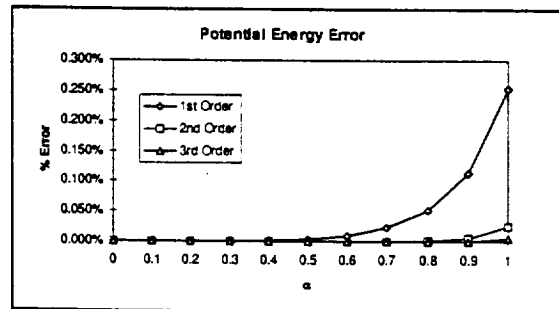


Figure 2: Potential Energy Error vs. Damage Magnitude.

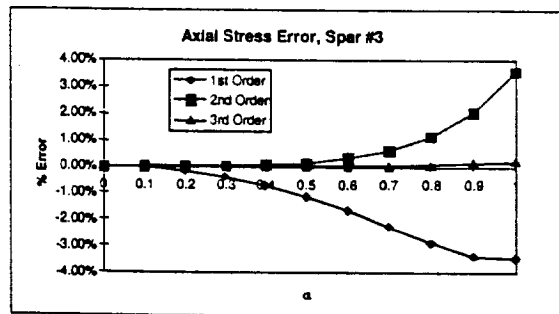


Figure 3: Axial Stress Error vs. Damage Magnitude.

Stress errors were also checked for elements that went through large changes in stress due to nearby damage. Figure 3 shows the axial stress error in a spar cap #3. Spar cap #3 is located in the vicinity of the damaged area (see figure 1). Both the first and second order approximations show reasonable accuracy; however, the third order approximation clearly indicates superior accuracy for this bar element.

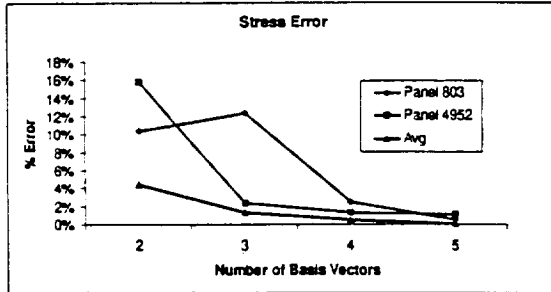


Figure 6: Representative Stress Errors

The accuracy of the approximation for stress is shown in Figure 6. The percent relative error to a complete reanalysis is illustrated versus the number of displacement response basis vectors. The average von Mises stress error of all panel elements is shown along with the stress error for two panels, which are located in design region two in the vicinity of the damage. These surface panels are considered good indicators of the performance of the approximations for the optimal design because their stress constraints are active (i.e., greater than -0.1). They exhibit large errors for 2 and 3 basis vectors, but they indicate good accuracy using 4 and 5 basis vectors.

The relative stress error for panel 803 shows a slight increase when using three basis vectors compared to two basis vectors. This is counter-intuitive to the general trend of expected increasing accuracy when using more terms in a series approximation. The increasing error for this element is a local phenomenon and can be attributed to low quality basis vectors. When the fourth basis vector is included in the approximation, the combination of these four basis vectors adequately approximates the displacements in the region of panel 803.

The relative errors for the stress sensitivity of several critical web elements are shown in Figure 7. These elements showed the largest relative error for elements having logarithmic derivatives greater than 0.2 and active stress constraints. The sensitivity is with respect to the face sheet thickness of an element located in

design region two in the vicinity of the damage. The average sensitivity error for elements with active stress constraints was 0.018, 0.013, 0.011, and 0.011 for 2, 3, 4, and 5 displacement response basis vectors, respectively. Although the average errors are small and insensitive to the number of displacement response basis vectors, individual element sensitivity results are sensitive to the number of basis vectors (Figure 7).

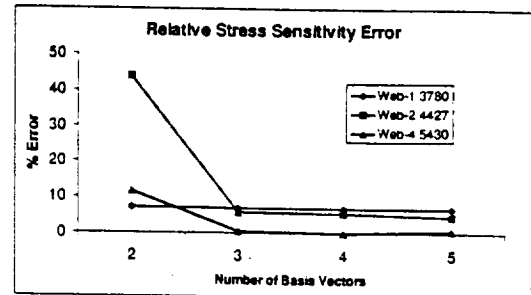


Figure 7: Representative Stress Sensitivity Errors

The box beam is optimized subject to both the undamaged condition with two load cases and five damage conditions. The basic damage conditions considered upper surface debonding, lower surface debonding, web debonding, upper spar cap chord fracture, and lower spar cap chord fracture, which were combined with the load cases to produce ten design conditions. The debonding considered 15-inch by 30-inch sections of the web, along with top and bottom skin panels. Two optimization runs were made. The first performed exact static analyses and semi-analytical calculations for each design cycle. The second used the CA approximations with 5 displacement response basis vectors for all damage design conditions (equation 3). CA based sensitivity approximations are done for damage conditions using the 5 displacement response basis vectors along with $u_{0,x}$ basis vectors (equation 11).

Execution times for a Silicon Graphics INDIGO-2 are summarized in Table 2. The load/damage condition is shown along with the CPU times in seconds for static analysis and sensitivity computations. The CPU times for the damage conditions are averaged for each load

Table 2: CPU Times (seconds) for Calculation of Design Constraints and Their Sensitivities.

Damage/Load Condition	Exact Static Analysis	Approx. Analysis	Exact Sens.	Approx. Sens.	Ratio Analysis	Ratio Sens.
2.5G Undamaged	751.25	731.71	633.29	629.91	0.97	0.99
2.5G Damage	609.00	98.07	410.88	151.65	0.16	0.37
-1.0G Undamaged	753.47	727.34	403.53	397.85	0.97	0.99
-1.0G Damage	608.74	98.04	410.42	150.61	0.16	0.37

condition. The CPU times for the CA approximation are compared to the CPU times for a complete reanalysis in this table for a single design iteration. The ratios of analysis times show a significant difference for the damage conditions, but are close to unity for each undamaged condition. This is due to the initial nominal static result required by the both the CA approximation and the exact analysis. The approximation shows significant computational savings for the damage conditions where reanalysis is required. It is also important to note that the ratio of sensitivity computation times do not show as great a computational savings as the static analysis. This is due primarily to the stress recovery stage of calculating the constraints and their sensitivities. This significant computational stage is identical for both the approximation and the exact reanalysis. Thus, the computational efficiency of the CA based sensitivity approximation is somewhat diluted.

Figure 8 shows the CPU times for exact and approximate damage optimization over the course of 20 iterations. In addition, it shows the objective function value for both the complete reanalysis and approximate reanalysis optimization runs over 20 iterations. (Note the expanded scale.) The box beam weight from the approximate optimization run was within 0.2% of the weight obtained using an exact reanalysis. In addition, no constraints were violated in either optimization run in the final design.

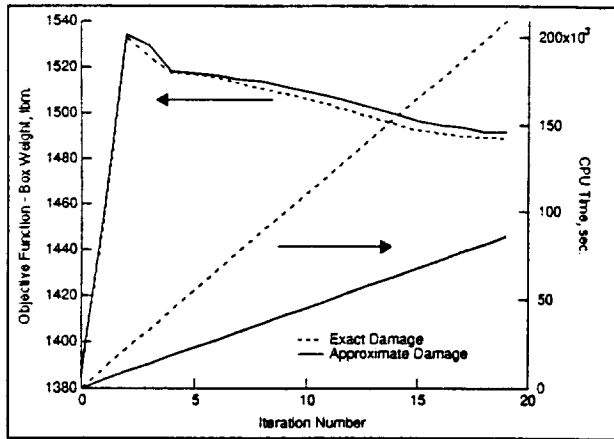


Figure 8: CPU Times and Objective Function Values.

The values of the design variables during the optimization were also examined. Figure 9 shows the lower surface spar cap areas, comparing the design variable values determined using a complete reanalysis and approximate reanalysis. Figure 10 shows the lower surface skin gauges. Figure 11 and Figure 12 show the upper surface skin gauges and lower spar cap areas, respectively.

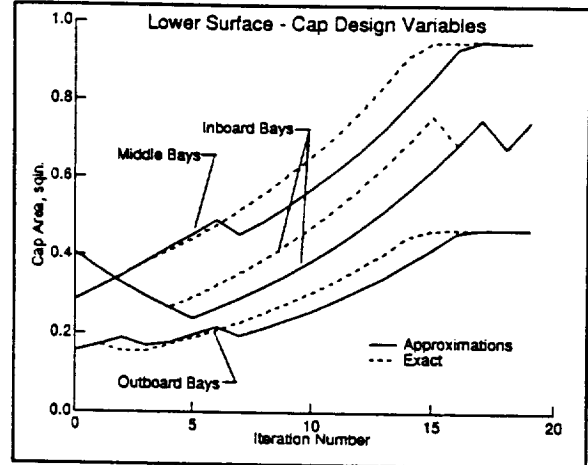


Figure 9: Lower Surface Spar Cap Areas

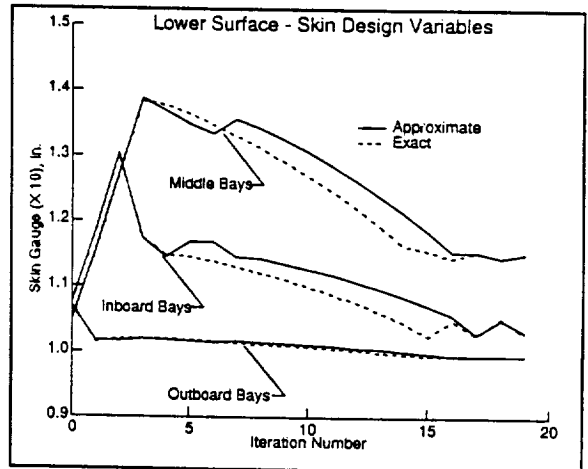


Figure 10: Lower Surface Skin Gauges

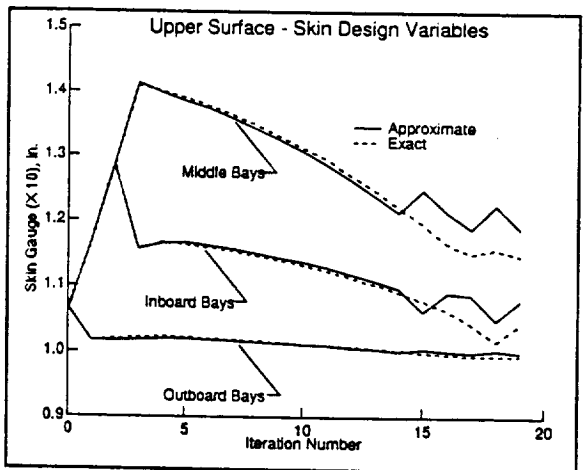


Figure 11: Upper Surface Skin Gauges

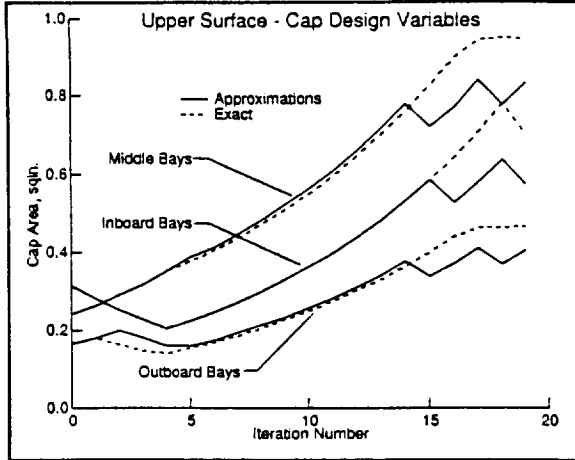


Figure 12: Upper Surface Spar Cap Areas

Many of the design variable values show some oscillations near the end of the optimization run. This phenomenon is likely caused by linearization of the problem, move limit size, and errors associated with the sensitivity calculations. Both the approximation to design derivatives for the damaged structure and the Taylor series approximation for the undamaged structure (see Appendix A) contribute. The value of the objective function is not significantly influenced by this phenomenon.

The basic premise of damage tolerant design is that a mass penalty is typically incurred if damage is not considered during optimization. When this box beam is optimized without considering damage, the resulting weight is 11% lighter than the damage tolerant design. However, when this lighter structure is damaged using the damage condition that generated the largest number of critical constraints, it can only carry 51.5% of the applied loading. These low values indicate the danger of substantial weight penalties for reinforcing the structure against damage after the fact.

Using the timing results from Table 2, the following formula has been developed to estimate the runtime savings using these approximations for structures similar in model complexity to the box beam:

$$R = \frac{lc_n(1 + 0.023 dv_n) + dc_n(0.137 + 0.009 dv_n)}{lc_n(1 + 0.023 dv_n) + dc_n(0.812 + 0.023 dv_n)}$$

where, R is the ratio of a single approximate design cycle to a single complete reanalysis design cycle; dv_n is the number of design variables; dc_n is the number of damage design conditions, and lc_n is the total number of load cases.

This formula was tested by modifying the box beam design problem for 8 design variables, 2 load cases, and 9 damage cases, which are combined into a total of 14 design conditions. The formula predicts a savings ratio of 0.341, where the actual comparison yields a ratio of 0.324. This formula can be expected to vary for other types of structures.

Conclusions

The case studies of the simple HSCT model and the detailed box beam show good accuracy for the CA approximation. The approximation reduced the cost of the analysis of a damaged box model by a factor of six and the cost of sensitivity by a factor of three. The lower efficiency of sensitivity calculations is due to the computational cost of stress recovery, which is common to both the approximation and exact derivative calculations. Overall, CPU time for the optimization was reduced by about a factor of two.

For complex structural models, using five basis vectors appears to provide good accuracy. Although the displacement response values are accurate for an approximation using three basis vectors, higher order approximations are required to yield accurate sensitivity values. Generation of each displacement response basis vector required approximately 2% of the computational cost of performing a single analysis, so using a high order approximation did not impose a significant penalty.

The runtime savings estimation lets designers assess the computational savings that these approximations provide. They can get a qualitative assessment of the computational cost of changing the number of design variables and the number of damage scenarios. For most damage tolerant airframe designs, a large number of damage scenarios (related to the number of load cases and design variables) would be typical in order to avoid designs tailored only to particular damage cases. The CA approximation makes damage tolerant design feasible by allowing designers to consider more damage cases and load cases in optimization problems by reducing the computational cost of each design cycle.

Acknowledgements

This work was supported in part by NASA cooperative agreement NCC-1260.

References

1 Barthelemy, J. -F. M., and Haftka, R. T., iApproximation Concepts for Optimum Design - A Review, i Structural Optimization, Vol. 5, 1993, pages 129 - 144.

2 Haftka, R. T., Starnes, J. H., and Nair, S., iDesign for Global Damage Tolerance and Associated Mass Penalties, i Journal of Aircraft, Vol. 20, No. 1, pp. 83 ñ 88, 1983.

3 Storaasli, O. O., and Sobieszczanski, J., iOn the Accuracy of Taylor Approximation, i AIAA Journal, Vol. 12, No. 2, pp. 231 ñ 233, 1974.

4 Noor, A. K., and Lowder, H. E., iApproximate Techniques of Structural Reanalysis, i Computers and Structures, Vol. 4, pp. 801 ñ 812, 1974.

5 Noor, A. K., and Lowder, H. E., iStructural Reanalysis via a Mixed Method, i Computers and Structures, Vol. 5, pp. 9 ñ 12, 1975.

6 Taye, S., iNorm Optimization Techniques for Improved Structural Reanalysis, i Computers and Structures, Vol. 41, No. 6, 1991.

7 Fox, R. L., and Miura, H., iAn Approximate Analysis Technique for Design Calculations, i AIAA Journal, Vol. 9, No. 1, pp. 177 ñ 179, 1971.

8 Kavanagh, K. T., iAn Approximate Algorithm for the Reanalysis of Structures by the Finite Element Method, i Computers and Structures, Vol. 2, pp. 713 ñ 722, 1972.

9 Kirsch, U., Effective Reanalysis of Structures, Concepts and Implementation, Technion, Department of Civil Engineering, January 1996.

10 Scotti, S. J., "Structural Design Using Equilibrium Programming Formulations," NASA TM 110175, June, 1995.

11 Whetstone, W. D., EISI-EAL Engineering Analysis Language Reference Manual, Volumes 1 & 2, EISI Inc., Mountain View, CA, 1983.

12 Whetstone, W. D., EAL333.11 Release Notes, EISI Inc., Mountain View, CA, May, 1996.

13 Haftka, R. T., Gürdal, Z., and Kamat, M. P., Elements of Structural Optimization, 3rd Edition, Kluwer Publishers, 1992.

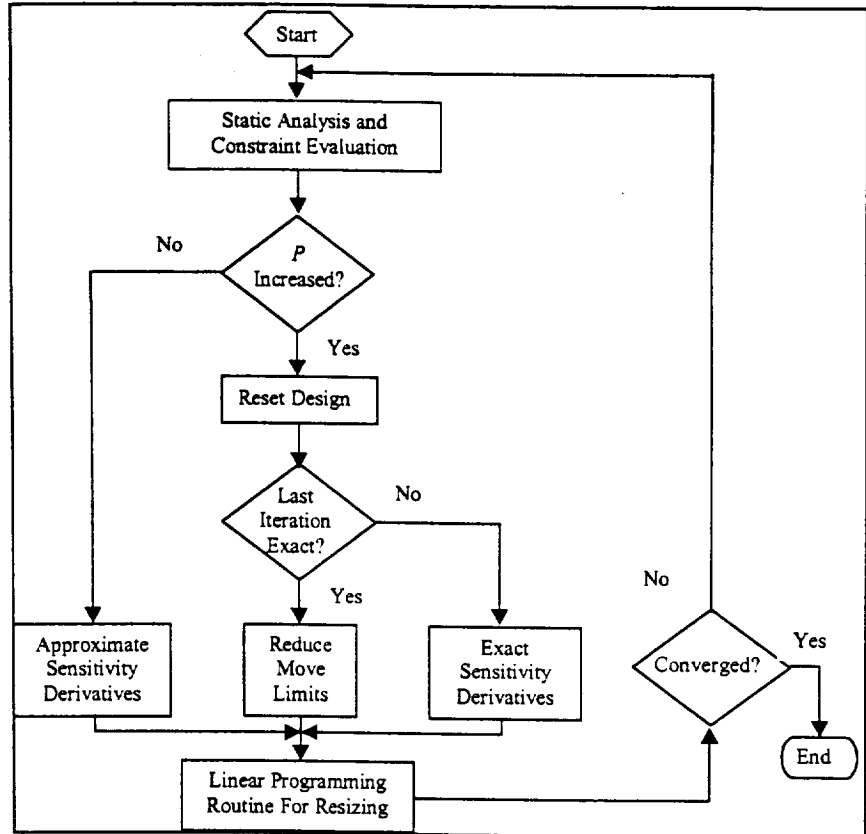


Figure 13: Flowchart of the Optimization Procedure

Appendix A

Since the response approximations discussed in this paper are added to the approximation used in the SLP procedure, we start by describing the basic procedure without the approximations for the damaged structures discussed in this paper. This basic SLP solution procedure is shown in the flowchart of Figure 13.

An iteration is represented by a circuit through the outermost loop. Iterations are either approximate or exact. An approximate iteration is defined as a pass through the outermost loop using approximate sensitivity derivatives. This approximation is described by Scotti¹⁰ and satisfies a second order Taylor series relation between the new and previous constraint sensitivities. An exact iteration is defined as a pass through the outermost loop using exact sensitivity derivatives, where the semi-analytic method is used for displacement derivatives, which are used in a first-order Taylor series to determine local, perturbed constraint values. Constraint derivatives are then determined by finite differences. In the present paper, the branch to the

“Approximate Sensitivity Derivatives” stage was disabled to better illustrate the effect of the damage approximation.

The optimization procedure is written primarily in the EAL command language with the addition of three external processors, which are written in FORTRAN.¹¹ Processors have been developed to evaluate stress and local buckling constraints for a number of structural sections common to aircraft design. Sequential linear programming using the MINOS V5.4 linear programming routine with move limits, as described by Scotti¹⁰, performs the optimization.

This procedure is now modified to incorporate the CA. instead of the exact analysis and sensitivity for damaged configurations.

Figure 14 shows the implementation of CA in the “Static Analysis and Constraint Evaluation” stage of the optimization procedure. Design conditions are made up from a load case and damage scenario. Multiple load cases and damage scenarios are allowed, and they may be combined in any way. Design conditions give a designer control over effectively matching critical load and damage situations. For design conditions with damage, the nominal state (u_0) is initially undamaged and is exactly solved before the effect of damage is approximated using CA, equations 3 - 8. Figure 15 shows the implementation of the approximation to design derivatives when calculating sensitivity derivatives, and replaces the “Exact Sensitivity Derivatives” stage in figure 13. It is important to note that the box titled “Semi-analytic/Approx. Constraint Derivatives” employs the same process shown in Figure 13 for an undamaged case. Our approximation to displacement derivatives, equations 15 - 18, is only used for damage scenarios, and constraint derivatives are obtained from displacement derivatives in the same manner as the undamaged case.

Figure 14: Static Analysis and Constraint Evaluation with Approximations

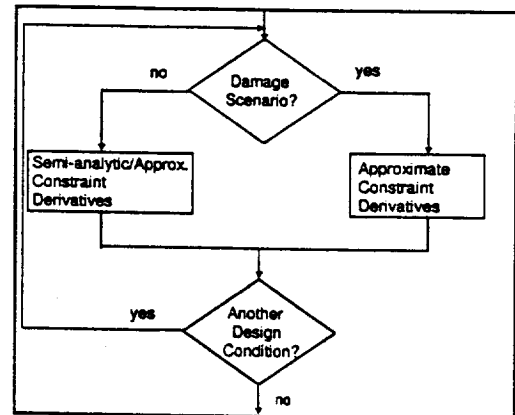
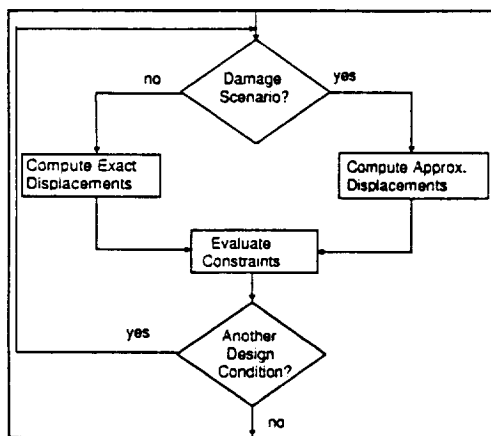


Figure 15: Calculation of Constraint Derivatives



**Adjoint Method for Sensitivity Calculations
In Damage Tolerant Design of Aircraft Structures**

Mehmet A. Akgün and Raphael T. Haftka

Department of Aerospace Engineering, Mechanics and Engineering Science

University of Florida, Gainesville, FL 32611-6250

Introduction

This addendum describes the work performed on the adjoint method of sensitivity calculation. The adjoint method is an alternative to the direct method and the finite difference method which are widely used. Finite difference derivatives are expensive computationally and prone to errors. The direct and adjoint methods are two classes of analytical sensitivity methods.

The adjoint method begins with calculation of an adjoint load, which depends on the particular response function of interest. It requires specialized programming for each type of response function, and this need has delayed its widespread application. However, for problems with multiple load cases or multiple structural configurations, such as damaged versions of a structure, the adjoint method can be much more efficient than the direct method. This computational advantage is enhanced for derivatives of stress functions because these derivatives can be calculated directly rather than obtained from derivatives of the displacements.

The objective of this part of the study was to lay the foundation for a demonstration of the advantage of the adjoint method for optimization under a variety of constraints. In particular, a condition was established that, when satisfied by stress and strain constraints, leads to a particularly easy implementation of the adjoint method. Applications with the von Mises stress limit, which is shown to satisfy this condition, are used as examples.

The Direct and Adjoint Methods

The discretized equations of equilibrium may be written in terms of the stiffness matrix \mathbf{K} , the force vector \mathbf{f} , and the displacement vector \mathbf{u} as

$$\mathbf{K}\mathbf{u}=\mathbf{f} \quad (1)$$

The recovery of the stress field σ from the displacement vector may be written as

$$\sigma =\mathbf{S}\mathbf{u} \quad (2)$$

When we differentiate these two equations with respect to a parameter p we get

$$\mathbf{K}\mathbf{u}_p=\mathbf{f}^p \equiv -\mathbf{K}_p\mathbf{u}, \quad \sigma_p=\mathbf{S}_p\mathbf{u}+\mathbf{S}\mathbf{u}_p \quad (3)$$

where subscript ' p ' denotes differentiation with respect to the design variable and \mathbf{f}^p is called the pseudo load. The direct method consists of calculating displacement and stress derivatives from Eq. (3). Because the matrix \mathbf{K} is available in factored form, the solution for displacement derivatives is much cheaper than the solution for the displacements. However, obtaining stress derivatives from displacement derivatives costs about the same as the original stress recovery, diluting the savings associated with the direct method compared to finite difference calculation. The method is easily implemented in finite element programs using finite difference evaluation of \mathbf{K}_p .

The adjoint method tackles directly derivatives of displacement functionals of the form $g(\mathbf{u},p)$. The derivative of g is given as

$$g_p=g_{,p}+g_{,u}\cdot\mathbf{u}_p \quad (4)$$

where a comma denotes a partial derivative with respect to the following subscript and a dot an inner product. With a bit of algebra, this can be converted into

$$g_p = g_{,p} + \mathbf{u}^a \cdot \mathbf{f}^p \quad (5)$$

where \mathbf{u}^a is the adjoint displacement field, found as a solution of the system

$$\mathbf{K}\mathbf{u}^a = g_{,u}^T \quad (6)$$

The direct method requires solutions of Eq. (3) for each design variable p , each load case, and each structural configuration. In contrast, the adjoint method needs to calculate derivatives of only potentially active constraints. The number of such constraints is of the order of the number of design variables. Consequently, when the number of load cases or structural configurations is large, the adjoint method is much more efficient than the direct method. Furthermore, it does not have to go through the stress recovery stage, translating displacement derivatives into stress derivatives.

However, there are implementation difficulties associated with the adjoint method, which prevent its wide-use application. The adjoint load vector $g_{,u}^T$ requires the derivatives of the response function with respect to displacement components. For stress components, or stress functions, such as the von Mises equivalent stress, $g_{,u}^T$ depends on the stress-displacement relationship, and hence on the details of the finite elements used. The information is not always readily available, and even when it is, the adjoint load must be programmed differently for each different finite element, an enormous programming burden. Fortunately, using a continuum formulation of the adjoint method instead of a discretized formulation can eliminate this burden.

Continuum Formulation of Stress Sensitivity

For the continuum approach, the stress function is more conveniently expressed as a stress functional G

$$G = \int g(\sigma, p) dV \quad (7)$$

where σ is a vector whose elements may be stresses or stress resultants. The integration typically represents an averaging process through a small volume of the structure. For a truss member σ is a scalar and is the axial force in the member. For a plane-stress element, σ is the vector of stress resultants, given by

$$\mathbf{N} \equiv \begin{bmatrix} N_x \\ N_y \\ N_{xy} \end{bmatrix} = t\mathbf{D} \begin{bmatrix} \varepsilon_x \\ \varepsilon_y \\ \gamma_{xy} \end{bmatrix} \quad (8)$$

where t is the plate thickness and \mathbf{D} is the constitutive matrix. The sensitivity of G to the design variable p is obtained by differentiating Eq. (7) with respect to p to yield

$$G_p = \int [g_{,p} + g_{,\sigma} \cdot (\sigma_{,p} + \sigma_{,\varepsilon} \varepsilon_p)] dV \quad (9)$$

where a dot indicates inner product, a subscript following a comma a partial derivative and that without a comma a total derivative. $p=t$ for a plane-stress element.

In this formulation, it can be shown (Haftka and Gürdal, 1992, p.314) that the adjoint load is an initial strain given by $g_{,\sigma}$ so that the loading depends on the stress function but not on the details of the finite element. This loading can be easily applied, then, in any program that has initial strain loading capabilities. Under the application of the adjoint load, the resulting displacement field is called the adjoint displacement \mathbf{u}^a . It can be shown that

$$G_p = \int (g_{,\rho} + \sigma_{,\rho} \cdot g_{,\sigma}) dV + \mathbf{f}^p \cdot \mathbf{u}^a \quad (10)$$

where \mathbf{f}^p is the pseudo load (Eq. 3). The integrand in Eq. (10) can be simplified under certain conditions. If g is a homogeneous function of degree n in its arguments, that is, if

$$g(c\sigma, cp) = c^n g(\sigma, p) \quad (11)$$

then it can be shown that

$$g_{,\sigma} \cdot \sigma + pg_{,\rho} = ng \quad (12)$$

If $n=0$, the constraint is unchanged (Eq. 11) when both the stresses σ and the design variable p are scaled up or down by the same factor. Here, the case where $n=0$ is of

importance since this applies to truss members and plane-stress elements as will be shown. The average stress in a truss member is given by

$$G = \frac{1}{L} \int \frac{N}{A} dL \quad (13)$$

where L is the length and A is the cross-sectional area. Similarly, the average von Mises stress in a plane-stress element is given by

$$G = \frac{1}{a} \int \sigma_{vM} da \quad (14)$$

where a is the surface area of the plate and σ_{vM} is the von Mises stress defined by

$$\sigma_{vM} \equiv \frac{\alpha}{\sigma_{yp}}; \quad \alpha \equiv \left[N_x^2 - N_x N_y + N_y^2 + 3N_{xy}^2 \right]^{1/2} \quad (15)$$

where σ_{yp} is the yield stress. In both Eqs. (13) and (14), the integrands are homogeneous to the 0th degree

Dividing Eq. (12) by p and keeping n for the time being,

$$g_{,\sigma} \cdot \frac{\sigma}{p} + g_{,p} = \frac{n}{p} g \quad (16)$$

If σ is such that $\sigma/p = \sigma_p$ then

$$g_{,\sigma} \cdot \sigma_{,p} + g_{,p} = \frac{n}{p} g \quad (17)$$

The condition on stress is satisfied for a truss member and a plate under in-plane loading when the design variables are the cross-sectional area and the plate thickness, respectively. For the latter element, for example, $N_t = N/t$ from Eq. (8).

Equation (10) hence becomes

$$G_p = \int \left(\frac{n}{p} g \right) dV + \mathbf{f}^p \cdot \mathbf{u}^a \quad (18)$$

When $n=0$, the integral in Eq. (18) disappears and the sensitivity is calculated easily. When n is non-zero, Eq. (18) is still easier to calculate than Eq. (10); the integrand is simply a multiple of the function g . Thus we find that for stress constraints in truss and membrane elements we have an additional simplification in the calculation of the derivatives.

The adjoint initial strain for a von Mises constraint is given by (Eqs. 14,15)

$$g_{,N}^T = \frac{1}{2\sigma_{yp}at\alpha} (2N - N') \quad (19)$$

where T denotes transpose and

$$\mathbf{N}' \equiv [N_y \quad N_x \quad -4N_{xy}]^T \quad (20)$$

Implementation in EAL

The adjoint approach has been implemented in EAL (Engineering Analysis Language), for von Mises stress constraints for plane-stress elements with thickness as the design variable. The initial strain (Eq. 19) is implemented via dislocations within each element whose stress sensitivity is sought. A runstream was written for this purpose. Simple plate structures having known solutions were analyzed with this runstream for verification. The results of this runstream were compared to those of the runstream written by Ed Jones of EISI and were seen to be identical. Ed Jones' approach, however, was found more suitable for automating the process for an arbitrary structural mesh and was therefore adopted from that point on. His runstream was modified and made more general.

The basic steps in sensitivity analysis with the adjoint method using EAL are the following:

- Given the stress state in the structure due to the external loading, calculate the initial strains to be imposed and the corresponding dislocations that would induce those strains in regions of the structure where sensitivity is sought, namely regions where constraints are critical.
- Apply the dislocations to the structure to compute the adjoint displacement vector \mathbf{u}^a .
- Compute the pseudo load \mathbf{f}^p comprising forces which, in the direct method, would be applied to the structure to solve for the response sensitivity \mathbf{u}_p , Eq. (3). The pseudo load vector consists mostly of zeros except for entries corresponding to the nodes of the element(s) whose thickness is being changed.
- Use \mathbf{u}^a and \mathbf{f}^p in Eq. (18) to compute the sensitivity.

The pseudo load can be computed in two ways:

- *From Eq. (3)*, which requires the derivative of the global stiffness matrix \mathbf{K} . That derivative can be obtained from finite difference and will be filled with zeros except for those entries corresponding to the modified element(s). The derivative will then be postmultiplied with the nominal displacement \mathbf{u} . Advantage can be taken of the sparse nature of \mathbf{K}_p .
- *From a continuum approach*. \mathbf{f}^p is the load which induces a strain field of $-\varepsilon/t$ in the modified element(s) with ε being the strain state in the nominal structure due to the external loads (Haftka and Gürdal, 1992, p. 309). As such, the problem here is not different from imposing an initial strain that causes adjoint displacements. Hence, dislocations can be computed corresponding to $-\varepsilon/t$ and, in turn, proceeding one step further, equivalent nodal forces corresponding to these dislocations. The latter forces will be the pseudo loads.

The preceding steps were implemented in a simple model of high speed civil transport (HSCT). The pseudo loads were computed with the continuum approach. The first and the second approaches were checked against each other with a simpler plate structure. Analysis runs were made with the HSCT model under five load cases. Currently investigation is carried out of how various load cases govern stress constraints relative to each other throughout the structure.

A copy of the runstream that implements the adjoint method for triangular E31 elements in EAL is attached.

REFERENCE

Haftka, R. T. and Gürdal, Z., *Elements of Structural Optimization*, Kluwer Academic Publishers, 3rd edition, 1992.